1. AGENCY USE ONLY (Leave blank)	2. REPORT DATE	3. REPORT TYPE AND DATES COVERED
		FINAL/01 DEC 90 TO 31 JAN 94

4. TITLE AND SUBTITLE	5. FUNDING NUMBERS
MITHRAS STUDIES OF THE BOUNDARY BETWEEN OPEN AND CLOSED FILED LINES	

6. AUTHOR(S)

Dr de la Beaujardiere

2310/BS
F49620-92-C-0011

7. PERFORMING ORGANIZATION NAME(S) AND ADDRESS(ES)

SRI INTERNATIONAL
333 RAVENSWOOD AVE
MENLO PARK, CA 94025-3493

8. PERFORMING ORGANIZATION REPORT NUMBER

AFOSR-TR- 95 - 0 2 7 4

9. SPONSORING/MONITORING AGENCY NAME(S) AND ADDRESS(ES)

AFOSR/NM
110 DUNCAN AVE, SUTE B115
BOLLING AFB DC 20332-0001

DTIC
SELECTED
JUN 1 9 1995
F

10. SPONSORING/MONITORING AGENCY REPORT NUMBER

F49620-92-C-0011

11. SUPPLEMENTARY NOTES

"Original contains color plates: All DTIC reproductions will be in black and white"

12a. DISTRIBUTION CODE

APPROVED FOR PUBLIC RELEASE: DISTRIBUTION IS UNLIMITED

13. ABSTRACT (Maximum 200 words)

This project's mission is to study the underlying mechanisms that control the chain of coupling between the solar wind, magnetosphere and ionosphere. In the first year of this project, a study was initiated to determine the global response of the high-latitude ionosphere to forcing by magnetosphere substorms. An assimilative model was used with ground-based radar, magnetometer, and satellite measurements to differentiate substorms surge convection signatures form the ambient pre-substorm convection pattern. This study concluded that the perturbed convection pattern can be characterized by a small-scale two-cell "expansion" structure superimposed on a global-scale two cell pattern. The characterization of these intermediary potential patterns is an essential first step toward the creation of fully time-dependent polar convection models. Subsequent work on this project has focused on identifying ground-based techniques to determine the location of the open-closed field line boundary. Accurate determination of this boundary is required for studies of substorm evolution, for comparisons of polar cap to auroral zone on composition profiles for precise calculation of the reconnection electric field and for studies of global polar cap inflation and deflation. A summary description of the results from this new research follows.

DTIC QUALITY INSPECTED 5

15. NUMBER OF PAGES

16. PRICE CODE

17. SECURITY CLASSIFICATION OF REPORT	18. SECURITY CLASSIFICATION OF THIS PAGE	19. SECURITY CLASSIFICATION OF ABSTRACT	20. LIMITATION OF ABSTRACT
UNCLASSIFIED	UNCLASSIFIED	UNCLASSIFIED	SAR(SAME AS REPORT)

SRI International

Final Report • March 1995

MITHRAS STUDIES
OF THE BOUNDARY BETWEEN
OPEN AND CLOSED FIELD LINES

John D. Kelly, Program Manager
Richard A. Doe, Research Physicist
Geoscience and Engineering Center

SRI Project 3245

Prepared for:

Department of the Air Force
Air Force Office of Scientific Research
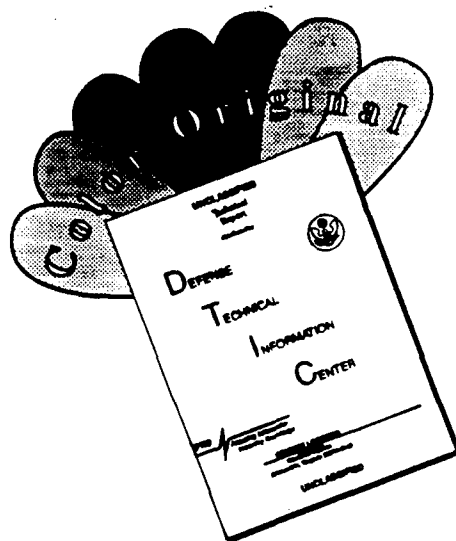Bolling Air Force Base
Washington, DC 20332

Attn: Major James Kroll
         Program Manager

Contract F49620-92-C-0011

19950615 014

DTIS QUALITY INSPECTED 5

DISCLAIMER NOTICE

THIS DOCUMENT IS BEST QUALITY AVAILABLE. THE COPY FURNISHED TO DTIC CONTAINED A SIGNIFICANT NUMBER OF COLOR PAGES WHICH DO NOT REPRODUCE LEGIBLY ON BLACK AND WHITE MICROFICHE.

MITHRAS STUDIES OF THE BOUNDARY BETWEEN OPEN AND CLOSED FIELD LINES

John D. Kelly, Program Manager
Richard A. Doe, Research Physicist
Geoscience and Engineering Center

SRI Project 3245

Prepared for:

Department of the Air Force
Air Force Office of Scientific Research
Bolling Air Force Base
Washington, DC 20332

Attn: Major James Kroll
         Program Manager

Contract F49620-92-C-0011

Approved:

James F. Vickrey, Director
Geoscience and Engineering Center

Murray J. Baron, Vice President
Advanced Development Division

Accesion For		
NTIS CRA&I		☒
DTIC TAB		☐
Unannounced		☐
Justification		
By		
Distribution /		
Availability Codes		
Dist	Avail and / or Special	
A-1		

TABLE OF CONTENTS

LIST OF ILLUSTRATIONS

LIST OF ABBREVIATIONS

AIC   auroral ionospheric cavity

CCD   charge coupled device

DMI   Danish Meteorological Institute

FAC   field-aligned current

IMF   interplanetary magnetic field

IRIS   imaging riometer for ionospheric studies

IS   incoherent scatter
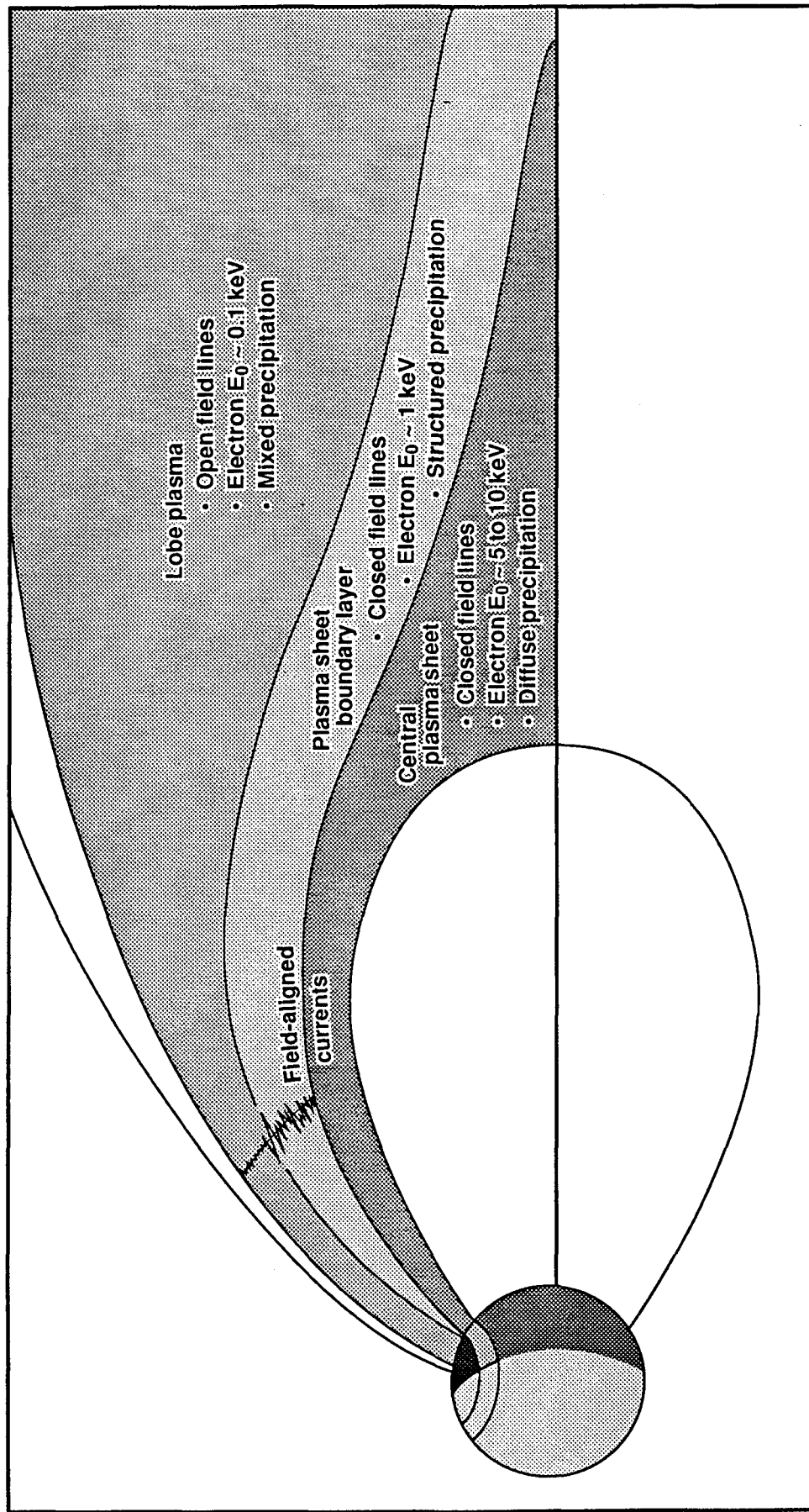
PSBL   plasma sheet boundary layer

1 INTRODUCTION

This project's mission is to study the underlying mechanisms that control the chain of coupling between the solar wind, magnetosphere and ionosphere. In the first year of this project, a study was initiated to determine the global response of the high-latitude ionosphere to forcing by magnetospheric substorms. An assimilative model [*Richmond and Kamide*, 1988] was used with ground-based radar, magnetometer, and satellite measurements to differentiate substorm surge convection signatures from the ambient pre-substorm convection pattern. This study concluded that the perturbed convection pattern can be characterized by a small-scale two-cell "expansion" structure superimposed on a global-scale two-cell pattern [*Kamide et al.*, 1994]. The characterization of these intermediary potential patterns is an essential first step toward the creation of fully time-dependent polar convection models.

Subsequent work on this project has focused on identifying ground-based techniques to determine the location of the open-closed field line boundary. Accurate determination of this boundary is required for studies of substorm evolution, for comparisons of polar cap to auroral zone ion composition profiles [*Kelly*, 1979], for precise calculation of the reconnection electric field [*de la Beaujardière et al.*, 1991], and for studies of global polar cap inflation and deflation [*Siscoe and Haung*, 1985]. A summary description of the results from this new research follows.

2 IDENTIFICATION OF THE POLAR CAP BOUNDARY

The nightside polar cap/auroral zone boundary, the surface that defines the transition from open to closed geomagnetic field lines, can also be characterized by a transition in plasma regimes and field-aligned current (FAC) signatures. Low and high altitude satellite data have shown that polar rain electrons in the open field line "lobe" region are typically cold (~ 100 eV) and isotropic [*Winningham and Heikkila*, 1974]; and they have shown that electrons in the closed field plasma sheet boundary layer (PSBL) region are typically hot and structured [*Winningham et al.*, 1975]. PSBL electron energy distributions also exhibit significantly more spectral structure than the typically Maxwellian energy distributions found in the lobe [*Newell et al.*, 1992]. Likewise, low altitude satellites have shown that FACs at lobe latitudes are often small and unstructured while PSBL FACs are much larger and highly structured [*Sugiura et al.*, 1984 and references within]. Figure 1 summarizes the juxtaposition of these topological, plasma, and current boundaries.

Satellite diagnostics have played a dominant role in deducing geomagnetic topology from plasma and electrodynamic signatures. Orbiting energetic particle detectors can unambiguously determine the energy distribution function, characteristic energy, integrated energy flux, and spatial structure associated with precipitating ions and electrons, and orbiting magnetometers can directly measure the structure of field-aligned current over the entire polar cap.

1

Lobe plasma
• Open field lines
• Electron E_0 ~ 0.1 keV
• Mixed precipitation

Plasma sheet boundary layer
• Closed field lines
• Electron E_0 ~ 1 keV
• Structured precipitation

Central plasma sheet
• Closed field lines
• Electron E_0 ~ 5 to 10 keV
• Diffuse precipitation

Field-aligned currents

Figure 1

GV95-006/v2-bw

Recurring satellite signatures for the nightside PSBL/lobe boundary include an absence of polar rain precipitation [Meng and Kroehl, 1977], a transition in number flux of energetic (> 1 keV) electrons [Frank and Craven, 1988], velocity dispersed ion structures [Zelenyi et al., 1990], and "region 0" downward currents [Burke et al., 1994]. Notable success has been achieved in automatically classifying dayside plasma regimes with the DMSP particle energy spectrograms with the aid of neural networks [Newell et al., 1991]. On the nightside, Robinson et al. [1992] have shown how satellite images at two UV wavelengths can be used to derive the mean energy of the precipitating electrons, a key discriminator for the PSBL/lobe boundary.

The central drawback to reliance on such satellite signatures is their limited temporal span and low duty cycle over the polar cap. Unlike the high-altitude DE-1 satellite, which measured the evolution of the polar cap over approximately 4 h periods, most energetic particle detectors are flown at lower altitudes (< 1000 km) with approximately 15 min of coverage over the polar cap. Such snapshots are especially difficult to interpret during periods when the polar cap boundary is in rapid motion. Satellite orbital mechanics dictate that the period between these short samples be as long as 90 min. Such long periods between samples can complicate coordination with ground-based diagnostics for studies of stochastic geophysical events such as substorms and transient polar cap arcs. For dynamic periods, the task of satellite/ground-based coordination becomes a variant of the human problem of "being at the right place at the right time."

High latitude ground-based diagnostics, on the other hand, can be thought of as executing 24 h period orbits *under* the polar ionosphere with the ability to sample at extremely high time resolution and with the ability to cover a wide range of latitudes and local times. For example, incoherent scatter (IS) radars can probe the ionospheric F region over a latitude range of 5° in approximately 3 min and allsky imagers can measure high-altitude emissions over a latitude range of 10° on a time scale as short as 20 s. Typical spatial resolutions at F region altitudes are approximately 0.1° of latitude for IS radar scan data and 0.02° of latitude for 6300 Å allsky images. Allsky imaging data, in particular, can describe the morphology of the distant polar cap boundary (at the southern edge of the image) prior to its eventual transit into the IS radar field of view. Such measurements of the polar cap boundary "time history" help guide the interpretation of IS radar measurements of large N_e gradients associated with the moving boundary.

In addition to ground-based allsky imagers and IS radars, imaging riometers and magnetometer chains can provide useful context measurements for IS radar and allsky imaging observations of the polar cap boundary. For example, the imaging riometer for ionospheric studies (IRIS) system provides a sky map of energetic electron impact over a 2° field of view [Hargreaves et al., 1991]. Although the threshold energy for these D region absorption events is too high to precisely detect the PSBP/lobe boundary (>20 keV), IRIS sky maps yield excellent latitudinal resolution and morphology for the hard precipitation events embedded within the PSBL proper. In contrast to the local nature of IRIS measurements, a magnetometer chain, such as the Danish

Meteorological Institute (DMI) array on the western coast of Greenland, provides an indication for the location and variability of auroral currents over nearly 20° of latitude [*McHenry et al.*, 1990]. Magnetometer chain data can therefore provide clues to the global evolution of current systems with approximately 1° of latitudinal resolution, a resolution unfortunately too coarse for precise location of the polar cap boundary.

An array of ground-based meridional scanning photometers can also be used to infer the location of the polar cap boundary [*Blanchard et al.*, 1995]. These authors choose to look for a step function gradient in 6300 Å emission with an amplitude at least 75% above that measured in the polar cap region. This method is well suited for real time boundary location but is judged to be too imprecise ($\pm 0.9^\circ$) to accurately locate the edge of the polar cap.

The study herein addresses the question of: to what extent can ground-based IS radar and monochromatic imagers be used to define plasma and FAC signatures associated with the nightside open-closed field line boundary. Detection of the boundary will be based on transitions in electron characteristic energy from typical PSBL to lobe values, and will be based on the observation of characteristic FAC signatures (see Section 3.1). This study will also examine the validity of specific radar/imaging techniques for use when the polar cap boundary is in rapid motion. A short review of relevant radar and imaging techniques used to discern this boundary and case study periods follow. The overall goal of this work is to bound the confidence associated with a single (or combinations of several) ground-based technique(s) in the absence of space-based diagnostics.

3 GROUND-BASED SIGNATURES FOR THE POLAR CAP BOUNDARY

3.1 RADAR SIGNATURES

IS radars have been traditionally used to search for auroral plasma regimes on the nightside by one of two methods: (1) by deriving the likely energy distribution of incident electrons from the shape of the low-altitude electron density profile [*Vondrak and Baron*, 1976; *Gattinger et al.*, 1991], and (2) by searching for E region plasma density above some *ad hoc* threshold level [*de la Beaujardière et al.*, 1991]. Both methods confine the IS radar beam to the plane of the magnetic meridian in order to describe the latitude of the boundary. A third method, isolating convection reversals in the ion flow pattern [*de la Beaujardière et al.*, 1987], has been shown unreliable on the nightside and will be ignored in the present discussion. Methods (1) and (2) seek to measure an ionospheric proxy for the characteristic energy and energy flux of the precipitating electron population. Two additional IS radar techniques described herein look for signatures associated with region 0 FACs: (3) detection of auroral ionospheric cavities (AICs) [*Doe et al.*, 1993], and (4) detection of electron temperature (T_e) enhancements in the F region [*Kagan et al.*, 1995].

The specific shape of E region electron density profiles can be used to reconstruct the energy distribution for the precipitating electrons by matching the radar derived ionization rate profile with a synthesized ionization profile derived from a superposition of monoenergetic electron beams [*Vondrak and Baron*, 1977]. This technique, referred to by its program name UNTANGLE, assumes that direct molecular recombination dominates plasma loss in the E region so that the ionization rate is proportional to the square of plasma density. The UNTANGLE method uses a modeled energy deposition profile to determine which monoenergetic beam will create significant ionization at a reference altitude, and then adjusts the number flux of the particular electron beam to match the radar-derived ionization rate. This process constructs a curve of differential number flux versus energy as the ionization profile is sampled over a range of altitudes from 80 to 200 km. The characteristic energy determined from this distribution can be used to infer the transition from PSBL to lobe plasma regimes. This method has been successfully used with elevation scan data to describe the latitudinal variation of electron energy across an auroral boundary arc (Figure 11, *Vondrak and Baron* [1977]).

An alternate method for determining characteristic energy and energy flux from N_e profile shape involves the creation of a library of synthesized ionization profiles based on assumed Maxwellian and Gaussian distributions for the precipitating electron population [*Gattinger et al.*, 1991; *Strickland et al.*, 1994]. This technique has the advantage of estimating contributions to total ionization from soft electrons with energies much less than 1 keV, and for differentiating diffuse polar cap profiles from structured auroral zone profiles. This method usually requires the IS radar to dwell at an angle looking up the local field line in order to ensure the recovery of high fidelity N_e profiles. Thus, one must wait for the boundary to move to magnetic zenith in order to determine its precise location. This procedure and the UNTANGLE procedure converge to similar derived energy distributions for moderately energetic ($>$ 500 eV) auroral profiles, and both methods are corroborated by comparison with dual-wavelength photometric techniques [*Vallance Jones et al.*, 1987; *Gattinger et al.*, 1991].

During periods of rapid expansion of the polar cap boundary, the IS radar can also search for N_e values in excess of an *ad hoc* threshold value, at an arbituary reference altitude (method 2 above). This technique is equivalent to searching for the PSBL/lobe boundary by isolating a single monoenergetic component of the total distribution. In the separatrix studies of *de la Beaujardière et al.* [1991] and *de la Beaujardière et al.* [1994], an assumed N_e threshold of 3×10^4 electrons cm^{-3} at 125 km and 150 km was used, respectively. These thresholds can be cast in terms of a field-aligned electron beam using an effective plasma recombination coefficient given by *Vickrey et al.* [1982] and the model ionization rate formulation of *Rees* [1989]. For the earlier study, the equivalent beam has an energy of 2 keV with an integrated number flux of approximately 1×10^7 electrons cm^{-2} s^{-1}, and for the latter study the equivalent beam has an energy of 800 eV with an integrated number flux of approximately 3×10^7 electrons cm^{-2} s^{-1}. While the choice of threshold N_e and

5

detection altitude had little effect on the conclusions reached in these specific studies, a more diffuse PSBL boundary region, corresponding to electrons with characteristic energy of less than 800 eV, would have been mistaken as a lobe region.

In addition to plasma signatures at the edge the nightside polar cap, evidence for unique FAC signatures has accumulated in recent years. Early suborbital rocket measurements of current sheets associated with auroral arcs suggested that downward FACs (carried by low energy electrons) are commonly found at the poleward edge of a system auroral arcs [*Cloutier et al.*, 1970; *Bryant et al.*, 1973; *Arnoldy*, 1974]. Later coordinated radar/satellite experiments have shown that a diverging electric field, which is the expected electrodynamic signature for a downward FAC, was observed at the boundary of the nightside auroral oval (as determined by AE-C satellite data) [*de la Beaujardière and Heelis*, 1984]. More recent radar/optical studies of boundary arcs, in regions presumably subject to enhanced reconnection, have postulated the closure of a magnetospherically imposed current pair [*Weber et al.*, 1991; *Gallagher et al.*, 1993]. In these two studies the downward component of the current system was located in the polar cap, poleward of the boundary arc. *Burke et al.* [1994] used low altitude DE-2 satellite data to conclude that such downward currents were coincident with the instantaneous PSBL/lobe boundary, and *Fujii et al.* [1994] used coordinated DE-1 and DE-2 data to conclude that this downward current is a persistent feature even during disturbed substorm periods.

In the absence of satellite magnetometer measurements, IS radar elevation scans can be used to identify downward FACs by detecting latitudinally narrow (~ 40 km), field-aligned depletions of the polar F region, so-called auroral ionospheric cavities [*Doe et al.*, 1993]. These AICs are thought to be the imprint of a magnetospherically imposed downward current filament that closes at the edge of an auroral arc. Satellite magnetometer measurements have confirmed that AICs form in regions of downward current, and coordinated IS radar/optical case studies have shown that AICs typically form in the same region in which region 0 nightside currents form: the poleward edge of the most poleward auroral zone arc. Plate 2 of *Doe et al.* [1993] illustrates an AIC located at the edge of bright ground-based and satellite imagery. For this example, *Robinson et al.* [1992] calculate an electron characteristic energy of 2.3 keV in the core of this boundary (presumably PSBL) arc and [*Doe et al.*, 1993] show that the AIC is collocated with a region of 1 μAm^{-2} downward current.

A related contextual signature of the FACs closing at the edge of the polar cap is a region of enhanced F-layer electron temperature detected poleward of the most poleward auroral zone arc. Such electron heating is unlikely to be due to precipitating electron impact as the T_e enhancement region is located several tens of kilometers poleward of the arc-related field line and is located in an area of ambient polar cap airglow emission [*Kagan et al.*, 1995]. These authors present a theory and supportive experimental evidence to show that electrons in the F layer are heated by collisional Alfvén waves that are in turn closely associated with the arc/cavity system of FACs. Because the efficiency of such Alfvén wave electron heating is proportional to the inverse square of plasma density, the presence of tenuous plasma in the polar cap F

layer or the presence of an AIC can increase the visibility of the heated region. Figure 2 illustrates a polar cap boundary scan with an arc/cavity pair and an associated F region T_e enhancement.

IS radar signatures of the polar cap boundary described thus far assume that a complimentary ground-based diagnostic, such as an allsky imager, has been used to verify the poleward transit of a system of auroral arcs into the radar field of view, and to verify the absence of significant arc signatures poleward of the boundary. In the following section we will examine how such allsky imagery can also corroborate radar estimates for the energetics of the precipitating electrons.

3.2 ALLSKY IMAGING SIGNATURES

Since the first International Geophysical Year (IGY, 1957-1958), broadband allsky auroral cameras have been used throughout the polar region to describe the two-dimensional horizontal context for various radiowave diagnostics of the high-latitude ionosphere. Such allsky images provided an indication for the orientation and morphology of auroral features over a range of latitudes from 5 to $10°$ depending on the centroid height assumed for the ensemble of individual emission lines. Measurements for the energy associated with aurora, on the other hand, were made by filtered photometers and spectrographs by looking up the local field line or scanning along the magnetic meridian.

Such photometer data from a series of NASA airborne optical campaigns in Alaska and the Canadian arctic allowed researchers to characterize magnetospheric source regions over a large range of latitudes and local times, based upon spectroscopic ratios as indicators of the mean energy of the precipitating electrons [*Eather and Mende*, 1972]. Data from this experimental campaign were also used by *Rees and Lummerzheim* [1989] to suggest that the spectral ratios of $N_2(2PG)$ to $N_2^+(1NG)$ (3371 Å/4278 Å) and of $O(^1D)$ to $N_2^+(1NG)$ (6300 Å/4278 Å) could both be used to predict electron characteristic energy. If one assumes that a Maxwellian population has been accelerated through a parallel potential, as would be expected in the PSBL region, then *Christensen et al.* [1987] argue that calibrated 6300 Å and 4278 Å data will yield characteristic energy, energy flux, and an estimate for upward field-aligned current. On the basis of coordinated radar/optical experiments, *Vallance Jones et al.* [1987] found good agreement between the characteristic energies derived from the UNTANGLE radar method and characteristic energies derived from the 6300 Å /4278 Å emission ratio.

Rapid advances in film emulsions, image intensifiers, and narrowband filters converged in the late 1970s to produce the first generation of monochromatic cameras capable of providing images for distinct emission species [*Mende and Eather*, 1976]. The advent of charge coupled device (CCD) technology allowed these allsky cameras to acquire and process images in a fully digital environment [*Baumgardner and Karandanis*, 1984]. Such digital processing enables accurate and repeatable correction
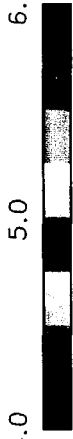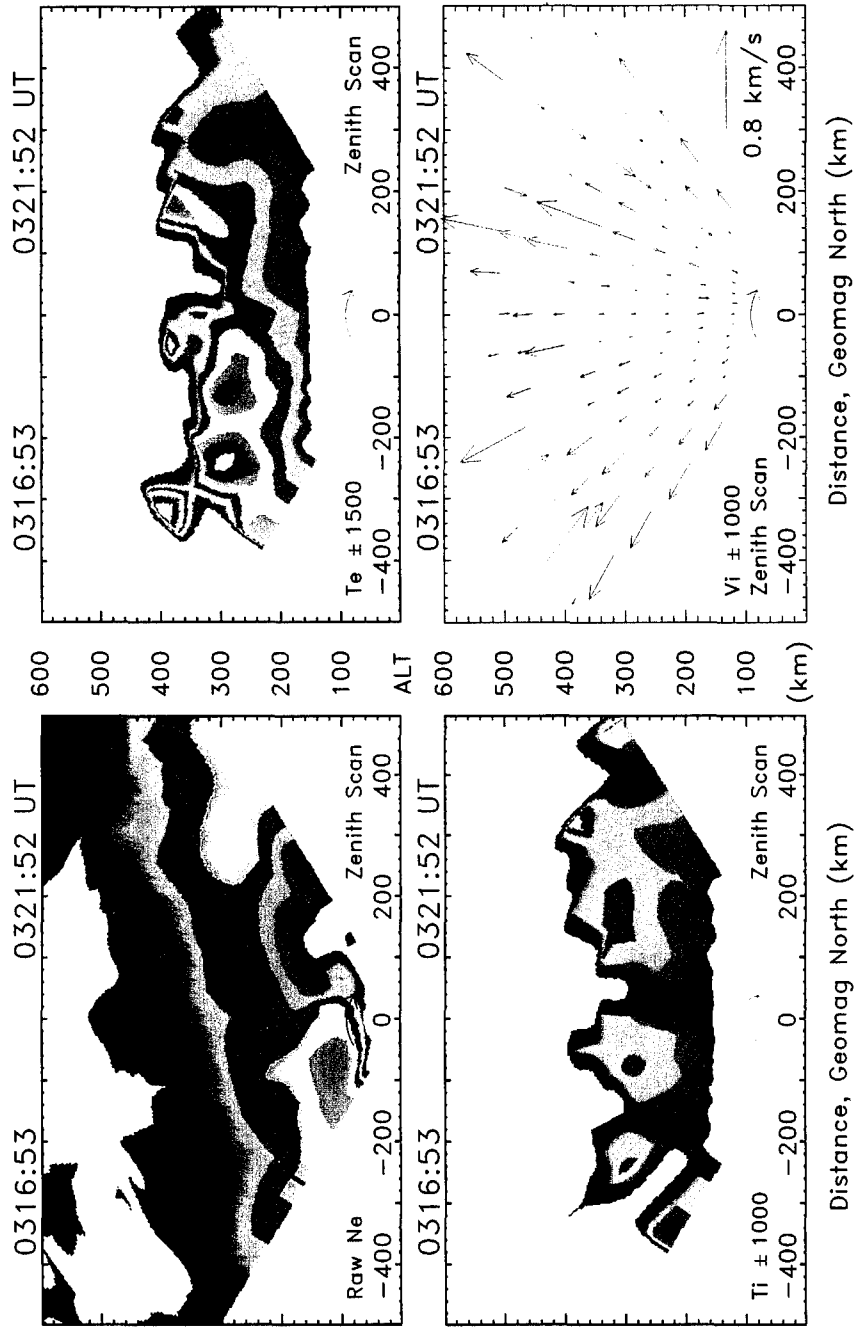
Figure 2

for CCD dark current noise, focal plane spatial inhomogeneities, field lens distortion, and off-band background contamination [*Oznovich et al.*, 1994].

This new class of auroral imager, or "imaging photometer," yields images that can be ascribed to a specific centroid emission altitude associated with a specific impact process [*Weber et al.*, 1991]. For example, the prompt 4278 Å emission line from N_2^+(1NG) can be ascribed to a height of 125 ±15 km, and the forbidden 6300 Å emission line from $O(^1D)$ can be ascribed to a height of 225±25 km (depending on the radar-derived N_e profile). Such emission centroiding allows the allsky images to be projected onto down-looking geographic and geomagnetic grids [*Weber et al.*, 1991; *Oznovich et al.*, 1994; *Doe et al.*, 1994].

The current study will use calibrated and geomagnetically mapped 4278 Å and 6300 Å images in order to form "red-to-blue ratio" images that will be subsequently rendered as images for the characteristic energy of polar cap boundary. The angular extent of these images will be limited to ±30° around zenith in order to avoid mapping distortions at the edge of the field of view. Figure 3 shows the process flow required to form the image of characteristic energy. This ratiometric analysis will be presented for a dynamic boundary arc and a stable boundary arc in Sections 4.1 and 4.3, respectively.

4 POLAR BOUNDARY CASE STUDY EVENTS

4.1 JANUARY 13, 1994

The first case study examines a dynamic and extremely energetic boundary arc observed subsequent to and following a substorm onset. This experiment coordinated measurements from the Sondrestrom IS radar facility in Greenland (lat. 66.99° N, long. 50.95° W) with a collocated allsky imager, an IRIS, and with the DMI magnetometer array.

Figure 4 shows a summary plot of 6300 Å allsky images during this event. For 1 h prior to the sudden auroral brightening at 0057:45 UT, the allsky imager recorded relatively dim ($\sim$ 200 Rayleighs) 6300 Å airglow over most of the optical field of view. Enhancements of this polar cap airglow were observed drifting in an antisunward direction in images from 0049:26 to 0054:58 UT; such patchlike enhancements are most likely a signature for interplanetary magnetic field (IMF) B_z south conditions in the polar cap [*Weber et al.*, 1986]. The apparent poleward velocity of the substorm surge can be calculated by projecting the allsky image into a geomagnetic reference frame [*Baker and Wing*, 1989] at an assumed emission altitude of 225 km and by locating the position of the 400 Rayleigh isophote in successive 6300 Å images. The resultant velocity of 560 m s^{-1} can be compared to a velocity estimate for the substorm-associated auroral electrojet derived from DMI magnetometer chain data.
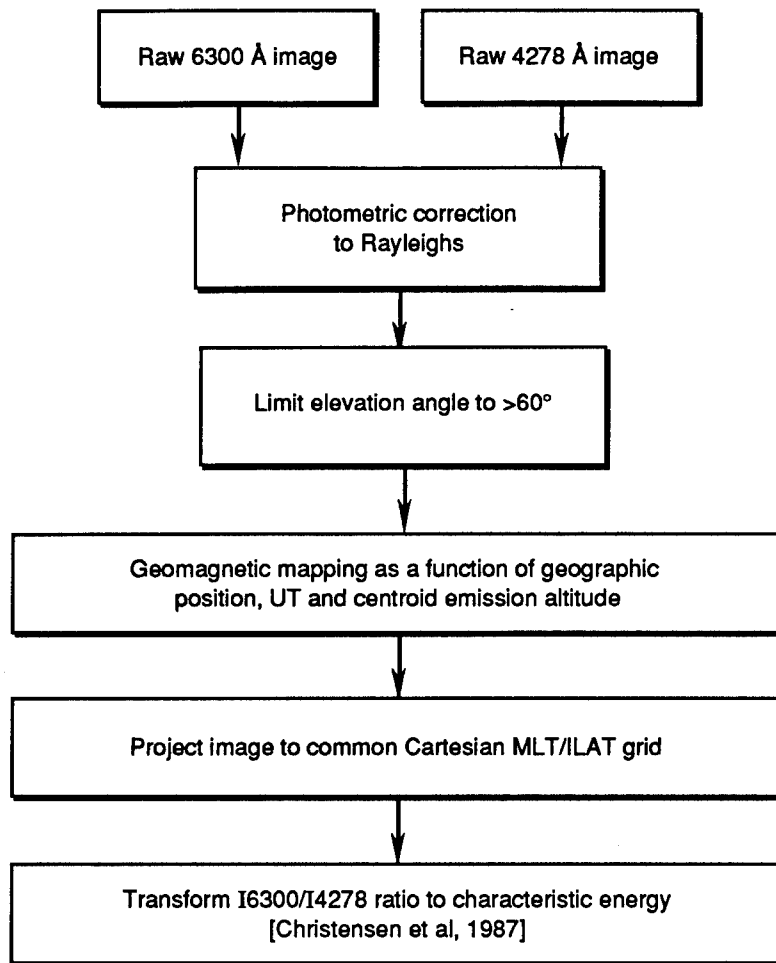
Figure 3   IMAGE PROCESSING TO OBTAIN E_0

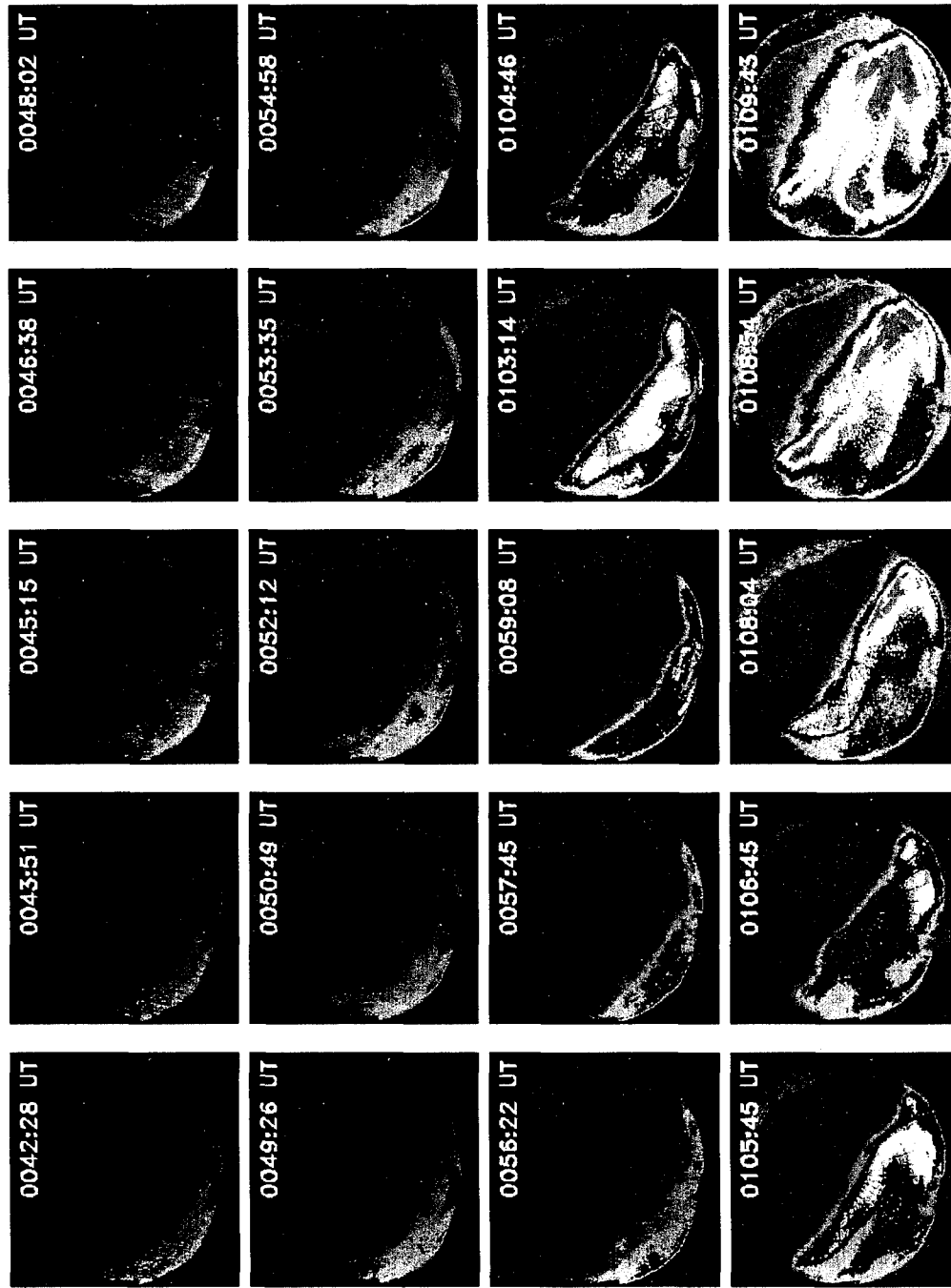LOCKHEED SONDRESTROM ALLSKY IMAGER RAW 6300 IMAGES   JAN 13, 1994

Figure 4

11

Figure 5 is a plot of north, east, and downward (H, D, and Z) components of the geomagnetic field from the western Greenland array. This plot shows a strong negative bay in the magnetometer H-component recorded at the Narssarssuaq (NAQ) station at approximately 0050 UT, corresponding to the intensification of an auroral electrojet current. This current system propagates poleward from Frederikshab (FHB, lat. 62° N) to Upernavik (UPN, lat. 72.8° N) in the subsequent 33 min period. This motion corresponds to an average velocity of 600 m s^{-1} and compares well with the 560 m s^{-1} velocity estimate derived from 6300 Å images. The arrival of the electrojet current over Sondrestrom also coincided well with observation of significant (> 2 dB) IRIS absorption. Thus the substorm current system, energetic electron impact, and associated optical emission are essentially collocated.

Figure 6 summarizes the evolution of N_e density structures during this period with a series of four elevation scans in the plane of the magnetic meridian. Prior imaging evidence for the existence of polar cap patches is now corroborated by observation of enhanced F region density structures in the first scan (0047:02 to 0051:41 UT). Line-of-sight velocities measured during the first three scans (not shown) indicate a bulk equatorward drift of 400 m s^{-1}. Poleward propagation of the aforementioned substorm current system within such a region of bulk equatorward drift satisfies the *Atkinson* [1986] observational criteria for a region undergoing enhanced reconnection.

The boundary arc in the last panel of Figure 6 was analyzed with the UNTANGLE procedure to determine the probable energy distribution of the associated precipi- tating population. The results of this analysis show that the N_e profiles measured through the central core of the arc, located 20 km south of radar zenith, would result from an electron population with a characteristic energy of 8 keV. The UNTANGLE analysis shows that the characteristic energy drops well below 1 keV at radar zenith. The precise location of the boundary arc can be determined at the point where the southward moving radar encountered the northward moving arc (fourth panel, Figure 6). The invariant latitude associated with the sharp arc gradient, as determined by the Polar Anglo-American Conjugate Experiment model [*Baker and Wing*, 1989], is determined to be 74.3°. Had the radar been scanning in the direction of arc transit, the precise location of the arc would have been impossible to determine.

Pairs of 6300 Å and 4278 Å images recorded during this period can be used to estimate the characteristic energy of this boundary arc using the ratiometric analysis described in Section 3.2. Such optical analysis yields a characteristic energy of 5 keV for the boundary arc and 200 eV for the zone poleward of the arc. The location of the boundary at the time when the IS radar beam illuminated the arc (0105:18 UT) can be determined by measuring the location for the 400 Rayleigh isophote in the 6300 Å image at 0104:46 UT, and advancing the boundary poleward by an increment corresponding to the product of the 560 m s^{-1} boundary velocity and 32 s time difference. The estimate for the location of the boundary using this method is 74.16°, in good agreement with the 74.3° estimate determined from the radar scan. We conclude that this boundary arc, which shows evidence for a region subject to enhanced reconnection, marks the instantaneous boundary of the polar cap.
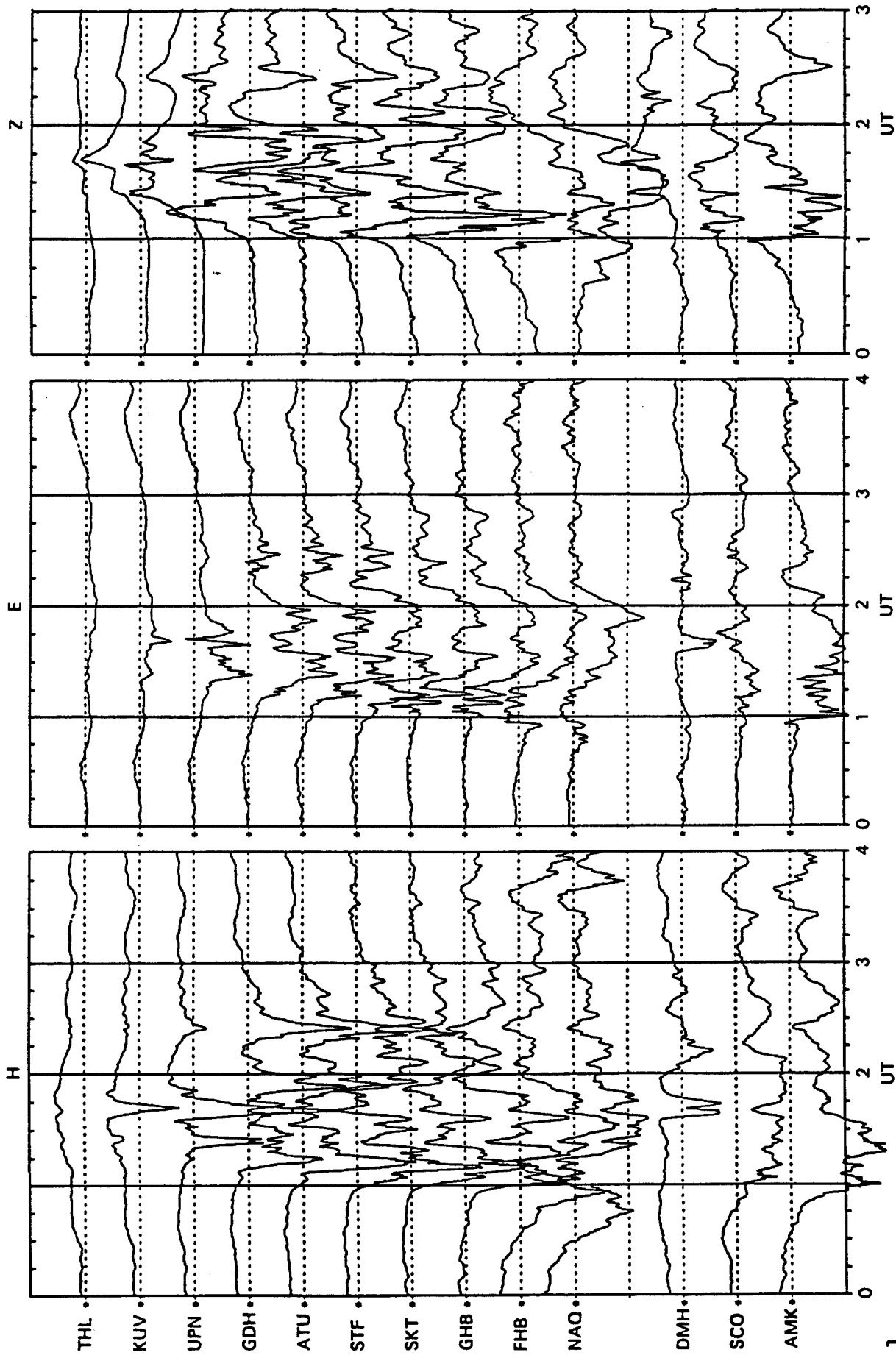
MAGNETOMETER CHAIN

GREENLAND

Figure 5

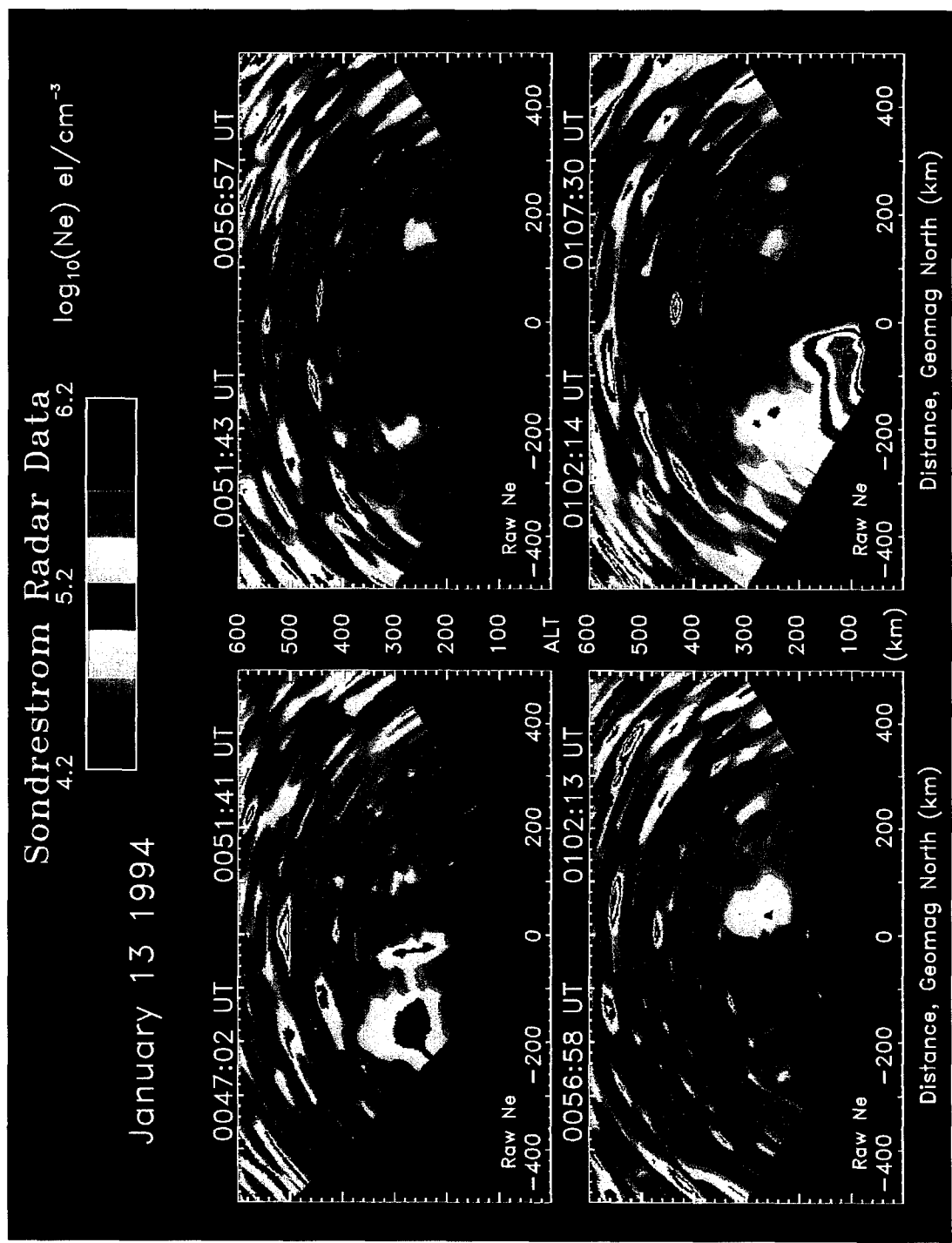300 nT   QL-TYPE 0   MY940111.GDF   D M I

13

Figure 6

4.2 JANUARY 11, 1994

The second case study examines an extremely stable auroral boundary for electrodynamic signatures of the PBSL/lobe boundary: AICs and enhanced F layer T_e regions poleward of an system of auroral zone arcs. Figure 7 shows a 15 min time history of 6300 Å allsky images corresponding to the transit of dense E region arc over the Sondrestrom radar. For this experiment the imager was used primarily as a context diagnostic and was therefore run at maximum duty cycle and without acquiring associated 4278 Å images. Thus, the ratiometric technique described in Section 3.2 could not be used for this period. For the 1 h period prior to the transit of this arc, significant auroral emission was observed only to the far south of the radar ($> 70°$ zenith distance) and the radar measured occasional patchlike N_e structures embedded in a relatively unstructured polar cap F layer.

Figure 8 shows a time series of six partial elevation scans gathered over a 12 min period when the arc first came into view. The local field line associated with the most dense leading edge portion of the approaching arc has been superimposed for reference. For each scan, the radar slewed from zenith to $45°$ elevation in the southern half plane of the magnetic meridian. This scan mode was designed to minimize the time required to move the radar to a fixed position looking straight up the local field line. While such a scan mode is advantageous for acquisition of high fidelity N_e profiles when the arc approaches magnetic zenith ($\sim 80°$ elevation), the mode truncated the bottom of the E layer arc for all but the last scan at 0310:47 UT. Such truncated profiles invalidate the UNTANGLE analysis for all but the last scan of the series at 0310:47 UT. Electron characteristic energy in the core of the arc during this scan is determined to be approximately 5 keV. Throughout this scan the radar was slewing southward during a time when the arc was moving slowly northward, and thus the polar cap boundary can be accurately located at $73.3°$ invariant latitude.

Close inspection of the radar N_e data reveals a field-aligned, relatively low density F region just poleward of the arc in every scan. These regions are depleted approximately 25% with respect to the average polar cap F region density of 10^5 electrons cm^{-3}, are latitudinally narrow (~ 30 km), and follow the motion of the arc boundary through this case study period. Such features satisfy the definition for auroral ionospheric cavities [*Doe et al.*, 1993] and indicate the likely presence of a downward FAC poleward of the arc system. In addition to this FAC signature, the final four panels of Figure 8 show regions of T_e elevated some $2000°$ K above ambient values. These heated regions are located poleward of the field line that threads the arc and are likely signatures of Alfvén wave heating of the polar cap F region of the type described by *Kagan et al.* [1995]. We contend that these additional radar signatures indicate the presence of a region 0 FAC and associated Alfvén wave at the PSBL/lobe boundary. These boundary signatures can be used to locate the polar cap boundary over the entire 12 min period of radar samples.
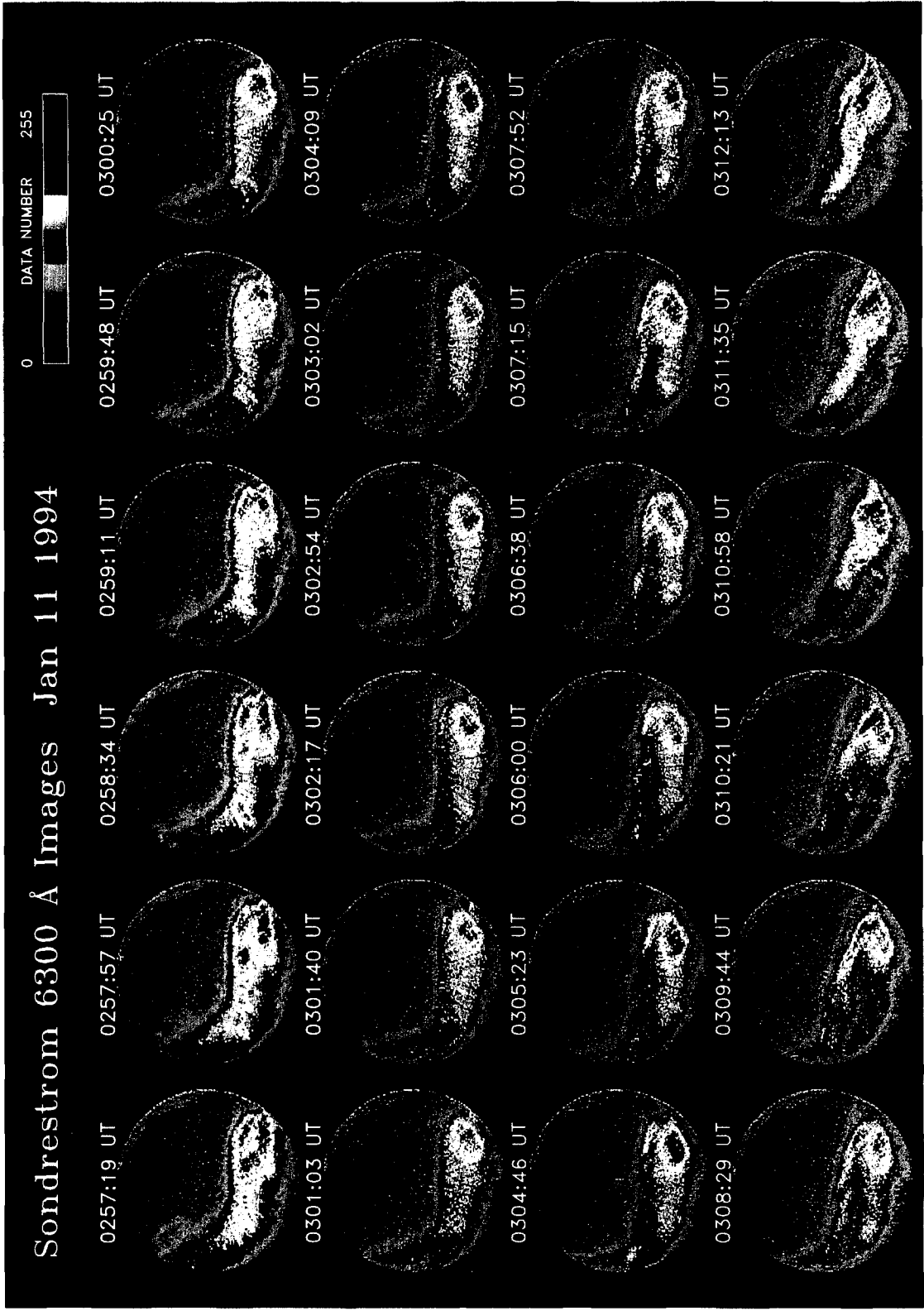
Sondrestrom 6300 Å Images Jan 11 1994
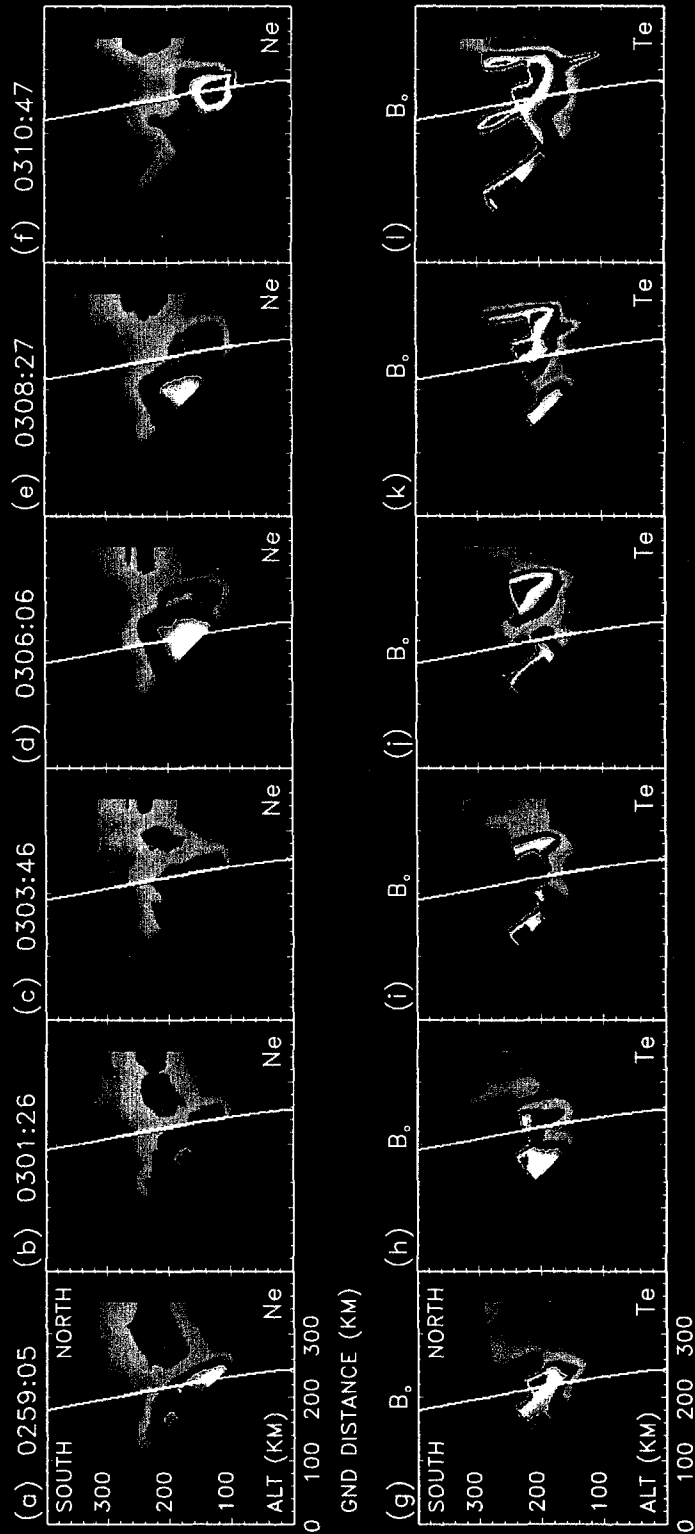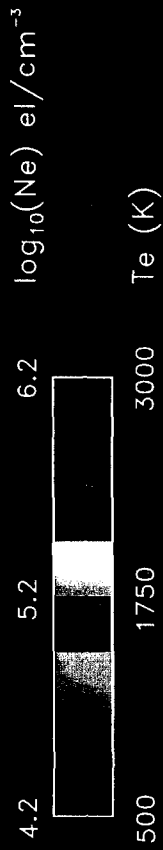
Figure 7

16

Figure 8

4.3 FEBRUARY 10, 1991

The third polar cap boundary case study examines a very stable boundary with IS radar data and two collocated allsky imagers. This period was geomagnetically quiet ($K_p = 2$) and the local Sondrestrom magnetometer indicated that a stationary auroral electrojet was present. This morningside boundary arc has been previously studied to detect ion velocity shears associated with the closure of FACs, to search for evidence of reconnection [*Gallagher et al.*, 1993], and to determine the horizontal convection pattern during periods of AIC formation [*Doe et al.*, 1994].

Figure 9 summarizes an 11 min period when the boundary arc remained at Sondrestrom's zenith with a series of paired allsky images at 6300 Å and 4278 Å. These data were recorded by the Air Force Phillips Laboratory allsky imaging photometer system. Two-wavelength images from the Boston University allsky imager were also acquired within 30 s of the times shown in Figure 9. Typical examples of data from the Boston University imaging system are shown in Plate 1 and Figure 4 of *Doe et al.* [1994]. Prior to 0340:14 UT, 6300 Å emission was located equatorward of zenith and occasional patchlike airglow enhancements were observed to drift equatorward from the northern half of the field of view.

IS radar data for this case study are summarized in Figure 10. The first and fourth panels show scans through the zenith and in the plane of the magnetic meridian (south is to the left). The second scan at 0343:08 UT is a scan through a plane that has been tilted to the west of the meridional plane by 30° in a manner described by *Weber et al.* [1991]. The third scan is similarly tilted to the east. These wing scans provide an indication that the boundary is longitudinally uniform over a 120 km range (at F region altitudes).

Line-of-sight ion velocity data (not shown) indicated that an equatorward bulk drift of approximately 300 m s^{-1} was observed during this period. This bulk drift agrees well with the relative motion of the large F region ionization patches observed in all four panels, and corroborate allsky indications of 6300 Å airglow enhancements. Although IMF data are not available during this period, the observation of such polar cap patches is an indication of IMF B$_z$ south conditions. *Gallagher et al.* [1993] derive a drift velocity of 350 m s^{-1} and note that the relative motion between the stationary arc and bulk convective drift is an indication of enhanced reconnection.

Figure 11 shows photometrically processed and geomagnetically mapped images for this boundary event. These images have been averaged over the scan time of the radar and have been limited to a 30° cone around zenith. At this point a red-to-blue ratio image can be formed by array division and this ratio image can be subsequently rendered as a map of characteristic energy using the formulation described by *Christensen et al.*, [1987]. Figure 12 shows the resultant image formed by this ratiometric analysis. A line plot of the characteristic energy along the central meridian (shown below the image in Figure 12) locates the poleward edge of the boundary arc at 74.5° invariant latitude, a location in excellent agreement with equatorward edge of the
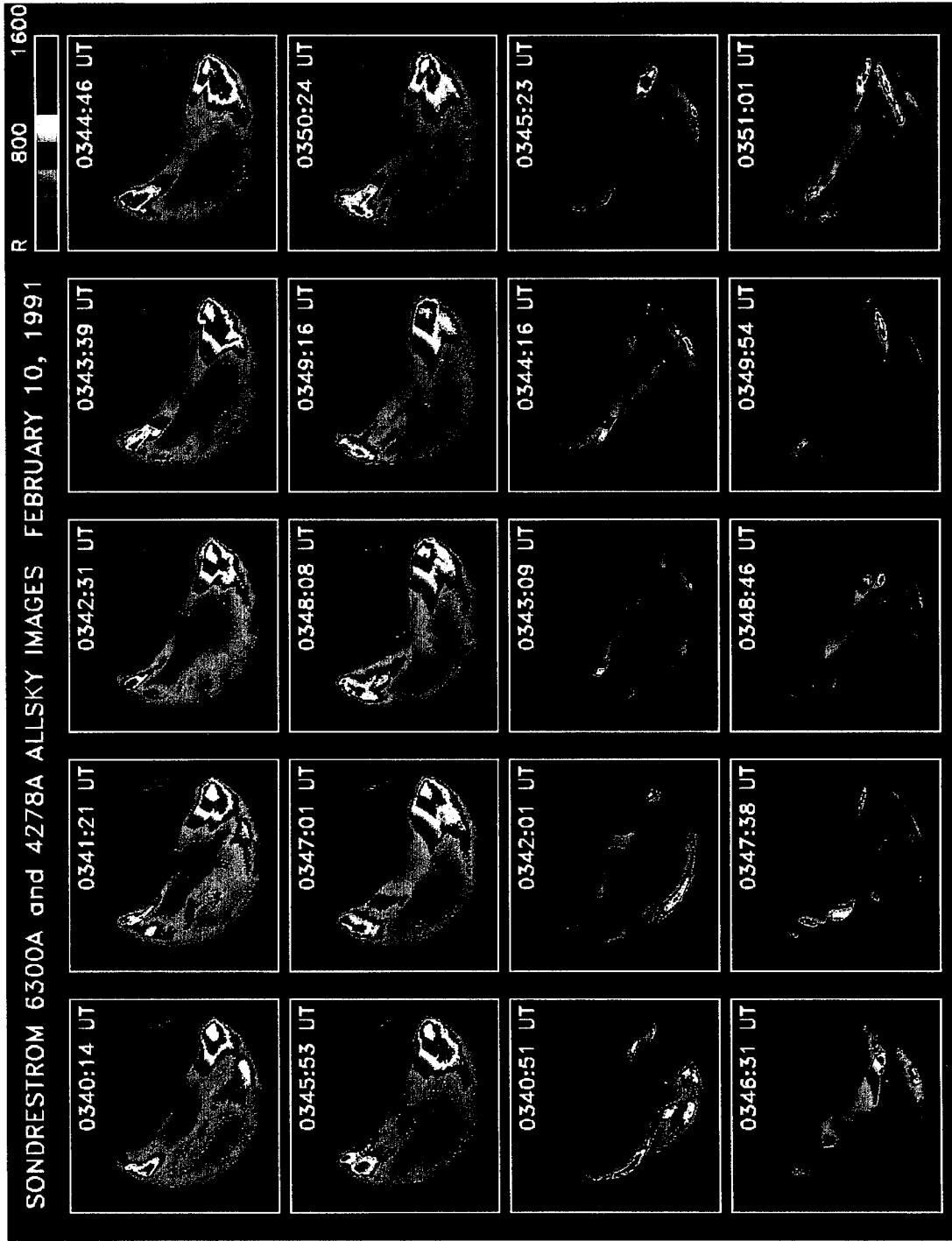
SONDRESTROM 6300A and 4278A ALLSKY IMAGES   FEBRUARY 10, 1991

Figure 9

Sondrestrom Radar

February 10 1991

$\log_{10}(Ne)$ el/cm^{-3}

Figure 10

Figure 11

Characteristic Energy

Feb 10, 1991
0347 UT

MLAT

Meridional E_0
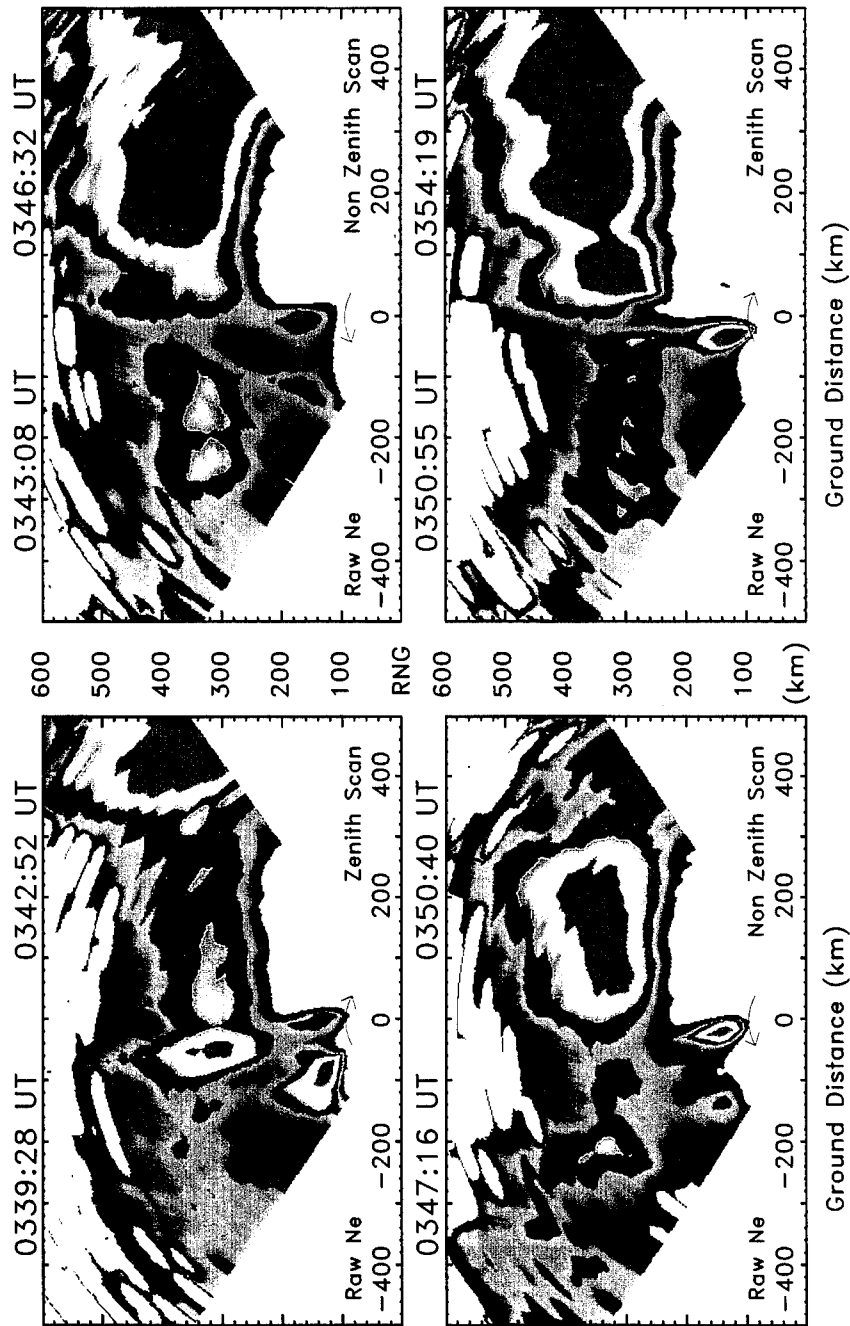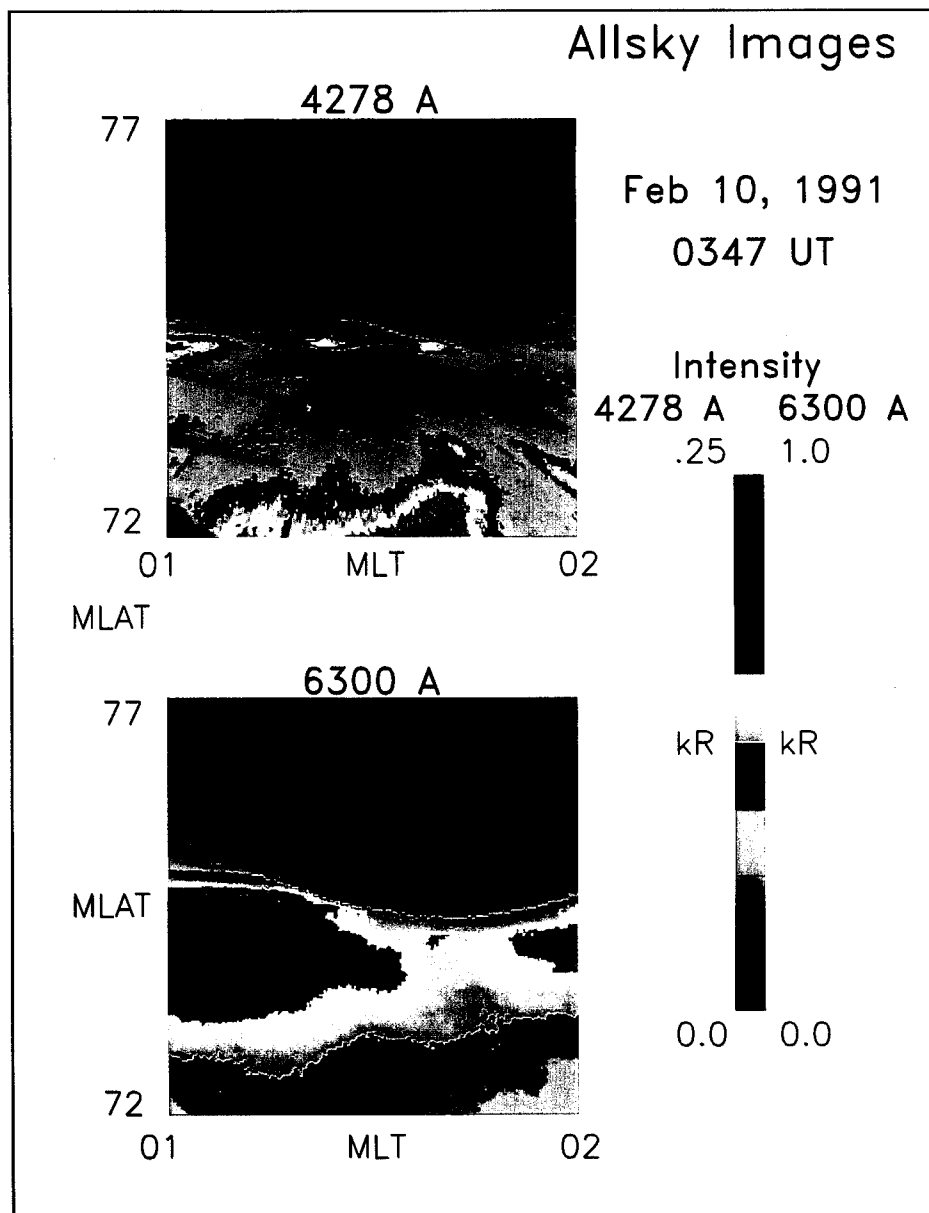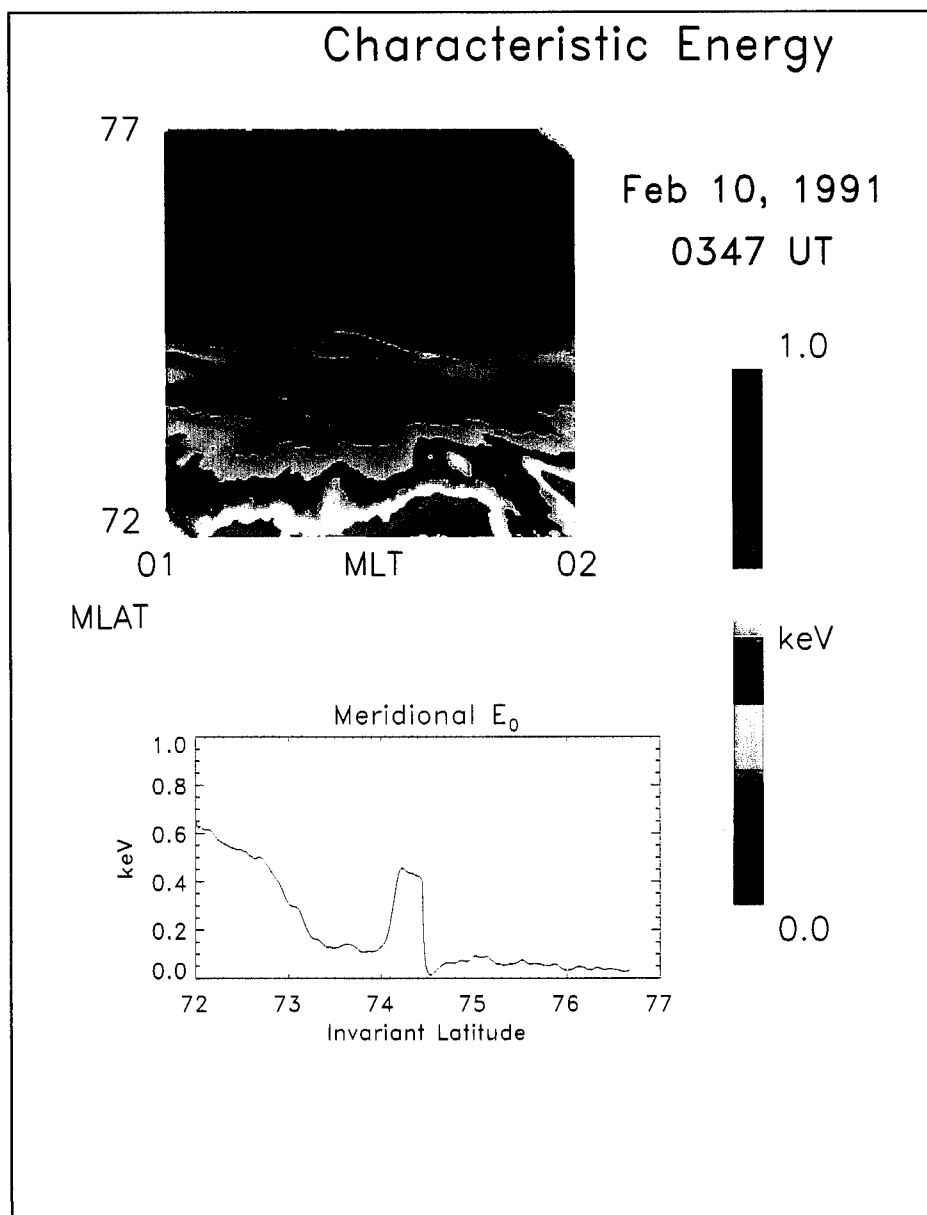
Figure 12

radar measured AIC ($74.4°$ invariant latitude). Unfortunately, the low energies associated with this arc preclude comparative assessment with the UNTANGLE method.

5 CONCLUSIONS

We have reviewed both IS radar and allsky imaging techniques for locating the polar cap boundary. The success of these methods hinges on the ability to differentiate the characteristic energy associated with PSBL and lobe regimes and on the ability to infer the presence of downward field-aligned currents. The confidence associated with IS radar determinations of this boundary must be weighted by the availability of contextual allsky imagery. For example, IS radar measurements of the characteristic energy across an arc boundary can only be related to the instantaneous polar cap edge by examining allsky images for the lack of significant emission poleward of the arc boundary. The time history of the polar cap boundary outside of the $5°$ F region radar field of view also helps guide the interpretation of radar scan data. Likewise, the radar data allow allsky images to be ascribed to an appropriate altitude for subsequent geomagnetic mapping.

The January 13, 1994, sudden substorm onset shows that both optical and radar methods can converge to a similar description for the energetics and location of the polar cap boundary. Although the UNTANGLE procedure locates the boundary arc at the point of radar beam intersection, the rapid motion of the substorm surge precludes an accurate radar estimate for the latitudinal dependence of electron energy across the polar cap boundary. The ability of the optical ratiometric technique to describe this boundary is only limited by the need for clear and moonless conditions. The February 10, 1991, case study shows how the optical technique can be used to render images for the spatial energy distribution across the entire boundary at energies below that required for UNTANGLE analysis. Finally, the January 11, 1994, case study shows how radar-derived signatures for FACs at the polar cap boundary can be used when the data set is inappropriate for UNTANGLE or ratiometric analysis.

23

6 REFERENCES

Arnoldy, R. L., "Auroral particle precipitation and Birkeland currents," *Rev. Geophys. Space Phys., 12*, 217-231, 1974.

Atkinson, G., "Verification of quantitative relationship among Birkeland current sheet motion, intensity and convective velocity, and also of criterion for expansive onset," *J. Geophys. Res., 91*, 8929, 1986.

Baker, K. B., and S. Wing, "A new magnetic coordinate system for conjugate studies at high latitudes," *J. Geophys. Res., 94*, 9139, 1989.

Baumgardner J., and S. Karandanis, "CCD system using video graphics controller," *Electronic Imaging, 3*, 28, 1984.

Blanchard, G. T., L. R. Lyons, J. C. Samson, and F. J. Rich, "Locating the polar cap boundary from observations of 6300 Å auroral emission," *J. Geophys. Res.*, in press, 1995.

Bryant, D. A., G. M. Courtier, and G. Bennett, "Electron intensities over two auroral arcs," *Planet. Space Sci., 21*, 165-177, 1973.

Burke, W. J., J. S. Machuzak, N. C. Maynard, E. M. Basinska, G. M. Erickson, R. A. Hoffman, J. A. Slavin, and W. B. Hanson, "Auroral ionospheric signatures of the plasma sheet boundary layer in the evening sector," *J. Geophys. Res., 99*, 2489, 1994.

Christensen, A. B., L. R. Lyons, J. H. Hecht, G. G. Sivjee, R. R. Meier and D. G. Strickland, "Magnetic field-aligned and electric field acceleration and the characteristics of the optical aurora," *J. Geophys. Res., 93*, 6163, 1987.

Cloutier, P. A., H. R. Anderson, R. J. Park, R. R. Vondrak, R. J. Spiger, and B. R. Sandel, "Detection of geomagnetically aligned currents associated with an auroral arc," *J. Geophys. Res., 75*, 2595, 1970.

de la Beaujardière, O., and R. A. Heelis, "Velocity spike at the edge of the auroral zone," *J. Geophys. Res., 89*, 1627, 1984.

de la Beaujardière, O., D. S. Evans, Y. Kamide, and R. P. Lepping, "Response of auroral oval precipitation and magnetospheric convection to changes in the interplanetary magnetic field," *Ann. Geophys., 5A*, 519, 1987.

de la Beaujardière, O., L. R. Lyons, and E. Friis-Christensen, "Sondrestrom radar measurements of the reconnection electric field," *J. Geophys. Res., 96*, 13907, 1991.

de la Beaujardière, O., L. R. Lyons, J. M. Ruohoniemi, E. Friis-Christensen, C. Danielsen, F. J. Rich, and P. T. Newell, "Quiet-time intesifications along the poleward auroral oval near midnight," *J. Geophys. Res., 99*, 287, 1994.

Doe, R. A., M. Mendillo, J. F. Vickrey, L. Zanetti, and R. Eastes, "Observations of nightside auroral cavities," *J. Geophys. Res., 98,* 293, 1993.

Doe, R. A., M. Mendillo, J. F. Vickrey, J. M. Ruohoniemi, and R. Greenwald, "Coordinated convection measurements in the vicinity of auroral cavities," *Radio Sci., 29,* 293, 1994.

Eather, R. H. and S. B. Mende, "Systematics in auroral energy spectra," *J. Geophys. Res., 77,* 660, 1972.

Frank, L. A. and J. D. Craven, "Imaging results from dynamics explorer 1," *Rev. Geophys., 26,* 249, 1988.

Fujii, R., R. A. Hoffman, P. C. Anderson, J. D. Craven, M. Sugiura, L. A. Frank, and N. C. Maynard, "Electrodynamic parameters in the nighttime sector during auroral substorms," *J. Geophys. Res., 99,* 6093, 1994.

Gallagher, H. A., E. J. Weber, J. F. Vickrey and R. L. Carovillano, "Plasma flows associated with an auroral arc at the polar cap boundary," *Auroral Plasma Dynamics, Geophys. Monogr. Ser., 80,* edited by R. L. Lysak, AGU, Washington, DC., 81, 1993.

Gattinger, R. L., A. Vallance Jones, J. H. Hecht, D. J. Strickland, and J. Kelly, "Comparison of ground-based optical observations of N_2 second positive to N_2^+ first negative emission ratios with electron precipitation energies inferred from the Sondre Stromfjord radar," *J. Geophys. Res., 96,* 11341, 1991.

Hargreaves, J. K., D. L. Detrick, and T. J. Rosenberg, "Space-time structure of auroral absoprtion events observed with the imaging riometer at south pole," *Radio Sci., 26,* 925, 1991.

Kagan, L., M. C. Kelley, and R. A. Doe, "Ionospheric Electron Heating by Alfvén Waves: Theory and Experiment," *J. Geophys. Res.,* submitted, 1995.

Kamide, Y., A. D. Richmond, C. F. Hutchins, B. A. Emery, B.-H. Ahn, O. de la Beaujardière, J. C. Foster, R. A. Heelis, H. W. Kroehl, F. J. Rich and J. A. Slavin, "Ground-based studies of ionospheric convection associated with substorm expansion," *J. Geophys. Res.,* in press, 1994.

Kelly, J. D., "Radar measurements of temperatures and ionic composition in the high-latitude ionosphere," Ph.D. dissertation, University of Alaska, Fairbanks, 1979.

McHenry, M. A., C. R. Clauer, E. Friis-Christensen, P. T. Newell, and J. D. Kelly, "Ground observations of magnetospheric boundary layer phenomena," *J. Geophys. Res., 95,* 14995, 1990.

Mende, S. B., and R. H. Eather, "Monochromatic all-sky observations and auroral precipitation patterns," *J. Geophys. Res., 81,* 3771, 1976.

Meng, C.-I., and H. W. Kroehl, "Intense uniform precipitation of low-energy electrons over the polar cap," *J. Geophys. Res., 82,* 2305, 1977.

Newell, P. T., S. Wing, C.-I. Meng, and V. Sigillito, "The auroral oval position, and intensity of precipitation from 1984 onward: an automated on-line data base," *J. Geophys. Res., 96,* 5877, 1991.

Newell, P. T., and C.-I. Meng, "Mapping the dayside ionosphere to the magnetosphere according to particle precipitation characteristics," *Geophys. Res. Lett., 19,* 609, 1992.

Oznovich, I., R. Yee, A. Schiffler, D. J. McEwen, and George J. Sofko, "The all-sky camera revitalized," *App. Optics, 33,* 7141, 1994.

Rees, M. H., and D. Lummerzheim, "Characteristics of auroral alectron precipitation derived from optical spectroscopy," *J. Geophys. Res., 94,* 6799, 1989.

Rees, M. H., *Physics and Chemistry of the Upper Atmosphere*, pp. 39-42, Cambridge University Press, Cambridge, 1989.

Richmond A. D., and Y. Kamide, "Mapping electrodynamic features of the high-latitude ionosphere from localized observations: technique," *J. Geophys. Res., 93,* 5741, 1988.

Robinson, R., T. Dabbs, J. Vickrey, R. Eastes, F. del Greco, R. Huffman, C. Meng, R. Daniell, D. Strickland, and R. Vondrak, "Coordinated measurements made by the Sondrestrom radar and the Polar Bear ultraviolet imager," *J. Geophys. Res., 97,* 2863, 1992.

Strickland, D. J., J. H. Hecht, A. B. Christensen, and J. Kelly, "Relationship between energy flux Q and mean energy $\langle E \rangle$ of auroral electron spectra based on radar data from the 1987 CEDAR campaign at Sondre Stromfjord, Greenland," *J. Geophys. Res., 99,* 19467, 1994.

Siscoe, G. L., and T. S. Huang, "Polar cap inflation and deflation," *J. Geophys. Res., 90,* 543, 1985.

Sugiura, M., T. Iyemori, R. A. Hoffman, N. C. Maynard, J. L. Burch, and J. D. Winningham, "Relationship between field-aligned currents, electric fields, and particle precipitation as observed by Dynamics Explorer-2," *Magnetospheric Currents, Geophys. Monogr. Ser., 28,* edited by T. A. Potemra, AGU, Washington, D. C., 96, 1984.

Vallance Jones, A., R. L. Gattinger, P. Shih, J. W. Meriwether, V. B. Wickwar, and J. D. Kelly, "Optical and radar characterization of a short-lived auroral event at high latitude," *J. Geophys. Res., 92,* 4575, 1987.

Vickrey, J. F., R. R. Vondrak, and S. J. Matthews, "Energy deposition by precipitating particles and joule dissipation in the auroral ionosphere," *J. Geophys. Res., 87,* 5184, 1982.

Vondrak, R. R., and M. J. Baron, "Radar measurements of the latitudinal variation of auroral ionization," *Radio Sci., 11,* 939, 1976.

Vondrak, R. R., and M. J. Baron, "A method of obtaining the energy distribution of auroral electrons from incoherent scatter radar measurements," *Radar Probing of the Auroral Plasma,* pp. 103-144, Universitetsforlaget, Tromsø-Oslo-Bergen, 1977.

Weber, E. J., J. A. Klobuchar, J. Buchau, H. C. Carlson, Jr., R. C. Livingston, O. de la Beaujardière, M. McCready, J. G. Moore, G. J. Bishop, "Polar cap *F* layer patches: structure and dynamics," *J. Geophys. Res., 91,* 12121, 1986.

Weber, E. J., J. F. Vickrey, H. Gallagher, L. Weiss, C. J. Heinselman, R. A. Heelis and M. C. Kelley, "Coordinated radar and optical measurements of stable auroral arcs at the polar cap boundary," *J. Geophys. Res., 96,* 17847, 1991

Winningham, J. D., and W. J. Heikkila, "Polar cap auroral electron fluxes observed with ISIS 1," *J. Geophys. Res., 79,* 949, 1974.

Winningham, J. D., F. Yasuhara, S.-I. Akasofu, and W. J. Heikkila, "The latitudinal morphology of 10-eV to 10-keV electron fluxes during magnetically quiet and disturbed times in the 2100-0300 MLT sector," *J. Geophys. Res., 80,* 3148, 1975.

Zelenyi, L. M., Kovarazkhin, R. A., and J. M. Bosqued, Velocity-dispersed ion beams in the nightside auroral zone: AUREOL-3 observations, *J. Geophys. Res., 95,* 12,119, 1990.